*Research Article*

# Numerical Analyses of Static Characteristics of Liquid Annular Seals Based on 2D LBM-LES Model

**Zhenjie Zhang,[1] Lulu Zhai [iD],[1,2] Jia Guo,[3] Zuchao Zhu,[1] and Guoyou Chen[2]**

[1]*State-Province Joint Engineering Lab of Fluid Transmission System Technology, Zhejiang Sci-Tech University, 928# No. 2 Avenue, Xiasha, Hangzhou, China*
[2]*Zhejiang Keer Pump Co., Ltd., Wenzhou, China*
[3]*Zhejiang Institute of Mechanical & Electrical Engineering Co., Ltd., Hangzhou, China*

Correspondence should be addressed to Lulu Zhai; zhailulu@zstu.edu.cn

Static characteristics and leakage flow rates of liquid annular seals have great influences on the hydraulic efficiency of turbomachinery. In this paper, a two-dimensional (2D) mathematical model for predicting the leakage flow rates and static characteristics of liquid seal is established, based on the lattice Boltzmann method (LBM) combined with the D2G9 velocity model for incompressible fluid and large eddy simulation (LES) turbulence model, in which the transformation equation of reference pressure is developed with the Bernoulli equation. Moreover, the proposed model is validated by comparing with the experimental results, calculation results based on the finite volume method (FVM), and the results based on the empirical method of three seals under different operating conditions. The comparisons show that the maximum deviation in leakage prediction of the calculating model based on 2D LBM is 4%, and this calculating model will effectively improve the leakage prediction accuracy of the seals compared with the FVM and theoretical method.

## 1. Introduction

In turbomachinery, there exist several sets of liquid annular seals, including neck-ring seals, interstage seals, and balance-piston seals. These seals prevent leakage flow while increasing the volumetric efficiency of the machinery. At present, there are mainly three methods to investigate the static and dynamic characteristics of these seals, including empirical formulas, bulk-flow method, and computational fluid dynamics (CFD) method. However, these three methods are all based on the hypothesis of continuous media, which means that the methods are all developed from a point of macroscopic view. With the development of the lattice Boltzmann method (LBM), many researchers started to use this method to solve different fluid flow problems of compressible and incompressible fluids. Compared with the widely used finite volume method (FVM), LBM has the advantages of simple algorithm, accurate calculation, and strong adaptability of boundary conditions, which also has provided an effective method for calculating fluid flow from a point of mesoscopic view. And in recent years, many researchers have analyzed the static and dynamic characteristics of sliding bearings, which are structurally similar to liquid annular seals based on LBM. Kucinschi and Afjeh [1] analyzed the internal flow characteristics and the fluid-film lubrication details within model sliding bearings based on 2D LBM. Kim et al. [2] have used LBM to study the flow conditions in a nano-sized air bearing, and Ramirez et al. [3] used this method to analyze the switching flow characteristics between different channels in a micron-sized air bearing. The simulation results showed that LBM has high accuracy in simulating the fluid flow of the sliding bearing with mini clearance.

Although the structures of sliding bearings are similar to those of liquid annular seals, there are major differences between them. The internal flow within sliding bearings is

laminar flow with small Reynolds number, while the internal flow of seals in the centrifugal pumps is highly turbulent with large Reynolds number. Recently, Posa and Lippolis [4], Li et al. [5], and Si et al. [6] analyzed the internal flow characteristics of centrifugal pumps considering liquid annular seals channels based on different turbulent models. Andres et al. [7], Saber and Abdou [8, 9], and Nagai et al. [10] proposed the theoretical calculation method for static and dynamic characteristics of different kinds of labyrinth seals and investigated the effects of operating conditions on these characteristics. As the maximum Reynolds number that fit the single-relaxation-time LBM (SRT-LBM) is $10^4$ and the maximum Reynolds number that fit the multiple relaxation-time LBM (MRT-LBM) [11] is $4 \times 10^4$, analyses on the fluid flow with large Reynolds number based on LBM are often performed with the turbulent model, such as LBM-k-$\varepsilon$ model established by Succi et al. [12], mixed length algebraic turbulent model established by Teixeira [13], and LBM-LES turbulent model established by Hou et al. [14]. However, the LBM-k-$\varepsilon$ turbulent model shows poor performances on describing flow separation, reattachment, and recovery effects [15], and mixed length algebraic turbulent model requires a large number of empirical coefficients, which make the two models not so widely used.

In contrast, the LBM-LES turbulence model combines the advantages of LBM and LES, in which the turbulent viscosity coefficient is calculated based on the Smargorinsky eddy viscosity model of LES. Premnath et al. [16] investigated the turbulent kinetic energy for the separation and attachment phenomenon of complex turbulent flow within a back-step model based on the LBM-LES turbulence model. Schneider et al. [17] used the LBM-LES turbulence model to solve the inlet flow characteristics of a centrifugal pump firstly. Chang et al. [18] analyzed the heat transfer between square cavity flow and back-step flow with the LBM-LES turbulent model. Comparisons between the numerical and experimental results showed that the method could describe the turbulent heat transfer flow well. Hamane et al. [19] simulated the flow within a 2D cylindrical channel with a large Reynolds number based on the LBM-LES turbulent model. Eitel et al. [20] introduced hierarchically refined lattice technology to the LBM-LES turbulent model and contrasted simulations of the cylinder flow model with different Reynolds number. The refinement of lattice reduced the number of lattice and significantly improved the computational efficiency. Nadim et al. [21] analyzed the flow of airfoil using LBM which combined the Smagorinsky SGS model, while parallel calculations were also used in the paper.

With the development of LBM, static characteristics and leakage analyses of liquid annular seals from a mesoscopic point of view become possible. In this paper, a two-dimensional (2D) mathematical model for predicting the leakage flow rates and static characteristics of liquid seal is established, based on the lattice Boltzmann method (LBM) and large eddy simulation (LES) turbulence model. Because the internal fluid of the seals is incompressible, the D2G9 velocity model for incompressible fluid is applied. Nonequilibrium extrapolation scheme is used for the boundary conditions of the wall.

Moreover, on comparisons of the experimental results with the results of LBM, FVM and empirical formulas are conducted and analyzed to verify the effectiveness and accuracy of LBM in calculating the results of static characteristics and leakages of seals.

## 2. Simulation Method

As the internal flow of the seal is mainly affected by the pressure-induced force, the lattice Boltzmann equation (LBE) can be expressed as follows:

$$\frac{\partial f}{\partial t} + c \bullet \nabla f = M(f). \tag{1}$$

In equation (1), $M$ is the rate of change from initial state to final state of the particle distribution function $f$, which is called collision operator. The basic thought of the Boltzmann equation is not to determine the motion state of each molecule but to find the probability of each molecule in a certain state and to obtain the macroscopic parameters of the system through statistical methods [22]. The distribution function $f$ acts to describe the number of molecules in a certain position in a certain range of speed at a particular time. The macroscopic values of velocity and pressure can be obtained by $f$, which is related to discrete velocity model, equilibrium distribution function, and its evolution equation [23].

*2.1. Governing Equations.* The governing equation of the LBM calculating model can be written as equation (2) under the SRT-LBM model. It has second-order accuracy at low Mach number. In equation (2), $\gamma$ is collision frequency, $\tau$ is relaxation time, and the relationship between $\gamma$ and $\tau$ is $\gamma = 1/\tau$. $\tau$ is mainly related to the lattice kinematic viscosity $\nu_0$ as shown in equation (3).

$$f_\alpha (x + c_\alpha \Delta t, y + c_\alpha \Delta t, t + \Delta t) - f_\alpha (x, y, t)$$
$$= -\gamma [f_\alpha (x, y, t) - f_\alpha^{eq} (x, y, t)], \tag{2}$$

$$\nu_0 = \frac{(2\tau - 1)}{6} \frac{(\Delta x)^2}{\Delta t}. \tag{3}$$

For the LBM calculating model, the distribution function evolution process is the most important component and the evolution process consists of two steps: the collision step that is described as equation (4) and the streaming step, which is described as equation (5).

$$f_\alpha (x, y, t + \Delta t) = f_\alpha (x, y, t)[1 - \gamma] + \gamma f_\alpha^{eq} (x, y, t), \tag{4}$$

$$f_\alpha (x + \Delta x, y + \Delta y, t + \Delta t) = f_\alpha (x, y, t + \Delta t). \tag{5}$$

*2.1.1. Discrete Velocity Model.* The discrete velocity model is one of the most important components of LBM calculating models. For compressible fluid flow calculation, Kataoka and Tsutahara [24] developed a new lattice Boltzmann velocity model for the compressible fluid simulation. Yang et al. [25]

studied the compressible fluid flow which is around NACA0012 airfoil by the D1Q4 velocity model. Yang analyzed the 3D viscous compressible flows [26] by using the lattice Boltzmann flux solver. Meanwhile, for incompressible fluid flow calculation, Qian et al. [27] established the D2Q9 velocity model for weakly compressible. In this model, fluid flow is driven by density gradient, and the relationship between pressure $P$ and $\rho$ is shown as equation (6). On the basis of the D2Q9 velocity model, Guo et al. [28] developed the D2G9 velocity model for incompressible fluid flow. The fluid flow is driven by pressure gradient in D2G9. The equilibrium distribution function satisfies $\Sigma f_\alpha^{\text{eq}} = \text{const}$. The macroscopic equations of the D2G9 velocity model can be derived by Chapman–Enskog expansion [29], and the equations can be written as equations (7) and (8) [28].

$$P = c_s^2 \rho, \tag{6}$$

$$\nabla \cdot u = 0, \tag{7}$$

$$\frac{\partial u}{\partial t} + \nabla \cdot (uu) = -\nabla p + \nu \nabla^2 u. \tag{8}$$

The form of equations (7) and (8) is equivalent to the incompressible Navier–Stokes equations.

In this paper, the D2G9 velocity model is used to solve the fluid flow within the liquid annular seals. The velocity directions of the model are shown in Figure 1. The speed configurations of the D2G9 model are shown as equation (9). where $e_a$ is the discrete velocity, $c$ is the lattice speed and it is defined as $c = \Delta x / \Delta t$, $\Delta x$ is the lattice step, and $\Delta t$ is the time increment.

$$e_\alpha = \begin{cases} (0,0), & \alpha = 0, \\ c\left(\cos\left[(\alpha-1)\dfrac{\pi}{2}\right], \ \sin\left[(\alpha-1)\dfrac{\pi}{2}\right]\right), & \alpha = 1,2,3,4, \\ \sqrt{2}\left(\cos\left[(2\alpha-1)\dfrac{\pi}{4}\right], \ \sin\left[(2\alpha-1)\dfrac{\pi}{4}\right]\right), & \alpha = 5,6,7,8, \end{cases} \tag{9}$$

### 2.1.2. Equilibrium Distribution Function.
The equilibrium distribution function of the D2G9 model is shown as equation (10). The equilibrium distribution itself is calculated from the macroscopic values which themselves are low order moments of $f$ [28].

$$f_\alpha^{\text{eq}} = \begin{cases} \rho_0 - 4d_0\dfrac{P}{c^2} + \rho_0 s_\alpha(u) & \alpha = 0, \\[2mm] d_1\dfrac{P}{c^2} + \rho_0 s_\alpha(u) & \alpha = 1,2,3,4, \\[2mm] d_2\dfrac{P}{c^2} + \rho_0 s_\alpha(u) & \alpha = 5,6,7,8, \end{cases} \tag{10}$$

$$s_\alpha(u) = \omega_\alpha \left[ \frac{e_\alpha \bullet u}{c_s^2} + \frac{(e_\alpha \bullet u)^2}{2c_s^4} - \frac{u^2}{2c_s^2} \right].$$
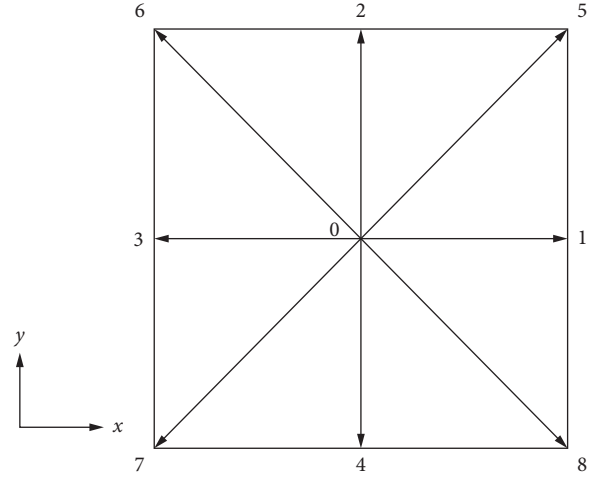


FIGURE 1: 2D, nine-velocity lattice direction.

In equation (10), the parameters $d_0$, $d_1$, and $d_2$ satisfy the relationship as equation (11) [28]. The macroscopic velocity and pressure equations can be given as equations (12) and (13), respectively.

$$\begin{cases} d_1 + d_2 = d_0, \\[2mm] d_1 + 2d_2 = \dfrac{1}{2}, \end{cases} \tag{11}$$

$$u = \frac{1}{\rho_0} \sum_\alpha e_\alpha f_\alpha^{\text{eq}}, \tag{12}$$

$$P' = \rho_0 \frac{c^2}{4d_0} \left[ \sum_{\alpha \neq 0} f_\alpha + s_0(u) \right]. \tag{13}$$

### 2.2. Turbulence Model.
According to the lattice Reynolds number equation shown as shown in equation (14), the lattice kinematic viscosity $\nu_0$ will decrease with the increase in Reynolds number. Since the flow within seals is highly turbulent with a Reynolds number of more than $10^4$, the relaxation factor $\tau$ is close to 0.5, which will make the computation difficult to converge. To solve this problem, the LBM calculating model combined with the 2D LES Smagorinsky model is established specially for the static characteristics and leakage of liquid annular seals. As shown in equation (15), the total lattice viscosity $\nu_t$ consists of two parts: the lattice kinematic viscosity $\nu_0$ and the Smargorinsky eddy viscosity $\nu_{t,LES}$. The value of $\nu_0$ can be described in equation (14), and the value of $\nu_{t,LES}$ is described in equation (16), in which $Cs$ is the Smagorinsky constant, $\Delta$ is the mean lattice spacing defined as $\Delta = (\Delta x \Delta y)^{1/2}$, and $\bar{s}_{ij}$ is the strain rate tensor that could be obtained by equation (17). In this paper, the value of Smagorinsky constant $Cs$ is fixed at 0.1 [18]. Besides, near the walls, $\nu_{t,LES}$ is damped, which means $\nu_{t,LES}$ will decrease and approach to zero as the wall is encountered.

$$\nu_0 = \frac{U_{\text{lattice}} \bullet H}{Re}, \tag{14}$$

$$\nu_t = \nu_0 + \nu_{t,LES}, \tag{15}$$

$$\nu_{t,LES} = (Cs\Delta)^2 \left| \bar{s}_{ij} \right|, \tag{16}$$

$$\bar{s}_{ij} = \sum_{\alpha=0}^{8} e_{\alpha i} e_{\alpha j} (f_\alpha - f_\alpha^{\text{eq}}). \tag{17}$$

### 2.3. Boundary Conditions.
Boundary conditions have great influences on accuracy, stability, and computational efficiency of LBM simulation. In this paper, velocity inlet, open outlet, and nonequilibrium extrapolation scheme are used as the initial boundary conditions.

#### 2.3.1. Velocity Boundary Condition.
The modified velocity boundaries based on bounce back part of the nonequilibrium extrapolation scheme are shown as equation (18). Extrapolation is used to calculate the outlet functions defined in equation (19) [30].

$$f_1(0, j) = f_3(0, j) + \frac{2}{3} p(0, j) u(0, j),$$

$$f_5(0, j) = f_7(0, j) - \frac{1}{2} [f_2(0, j) - f_4(0, j)] + \frac{1}{6} p(0, j) u(0, j),$$

$$f_8(0, j) = f_6(0, j) + \frac{1}{2} [f_2(0, j) - f_4(0, j)] + \frac{1}{6} p(0, j) u(0, j),$$

$$\tag{18}$$

$$f_{3,6,7}(NX, j) = 2 \bullet f_{3,6,7}(NX - 1, j) - f_{3,6,7}(NX - 2, j). \tag{19}$$

#### 2.3.2. Wall Boundary Condition.
Nonequilibrium extrapolation scheme [30] is chosen as the wall boundary condition. Pressure is used as the dynamic variable for eliminating compressibility errors in the simulation. As shown in Figure 2, Node $A$, Node $O$, and Node $C$ are located at the boundaries, and Node $E$, Node $B$, and Node $D$ are located in the flow field. The distribution function of the boundary Node $O$ can be calculated by the following equation:

$$f_\alpha(O, t) = f_\alpha^{\text{eq}}(O, t) + (1 - \gamma) [f_\alpha(B, t) - f_\alpha^{\text{eq}}(B, t)]. \tag{20}$$

### 2.4. Code Program.
Calculation code for leakage flow rate of liquid annular seals is accomplished by using C++ on the basis of 2D LBM combined with the governing equations, turbulence model, and boundary conditions described above. The overall program block diagram is shown in Figure 3.
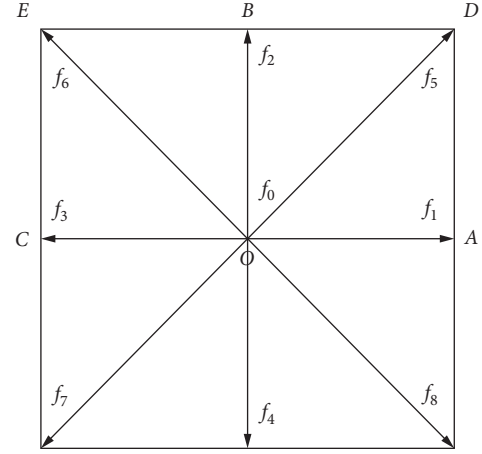


FIGURE 2: Nonequilibrium extrapolation equations.

## 3. Simulation Parameters

In order to verify the method proposed in this paper, the predicted leakage flow rates of three different liquid annular seals under different operating conditions based on LBM are compared with FVM results, experimental results, and theoretical results of empirical formulas. Figure 4 illustrates the basic geometry and coordinate system used in this paper. The geometric parameters of the three seals are listed in Table 1, and the operating conditions are illustrated in Table 2.

$$P = P_c - P_r = P_c - \frac{P'}{\rho_r u_r^2 / 2}. \tag{22}$$

### 3.1. Parameters of LBM.
The geometric parameters of model seals should be transformed to reference parameters with lattice unit [34], and the reference parameters must be the same value in the same model. The reference length $H_r$, reference velocity $u_r$, and reference density $\rho_r$ are defined as follows:

$$H_r = \frac{H'}{H},$$

$$\rho_r = \frac{\rho'}{\rho}, \tag{21}$$

$$u_r = \frac{c_s'}{c_s}.$$

In equation (21), where $c_s'$ and $c_s$ are the sound speed in physical unit and lattice unit, respectively, in this study, the value of $u_r$ is 2678.44 m/s. And $\rho'$ and $\rho$ are the density in physical unit and lattice unit, respectively; the value of the $\rho_r$ is 992 kg/m³. The reference length $H_r$ is defined by grid resolution; for example, if the lattice number of the model gets 9047 and the physical length $H'$ is 13.13 mm, the reference length $H_r$ should be $1.451 \times 10^{-6}$ m. Besides, the
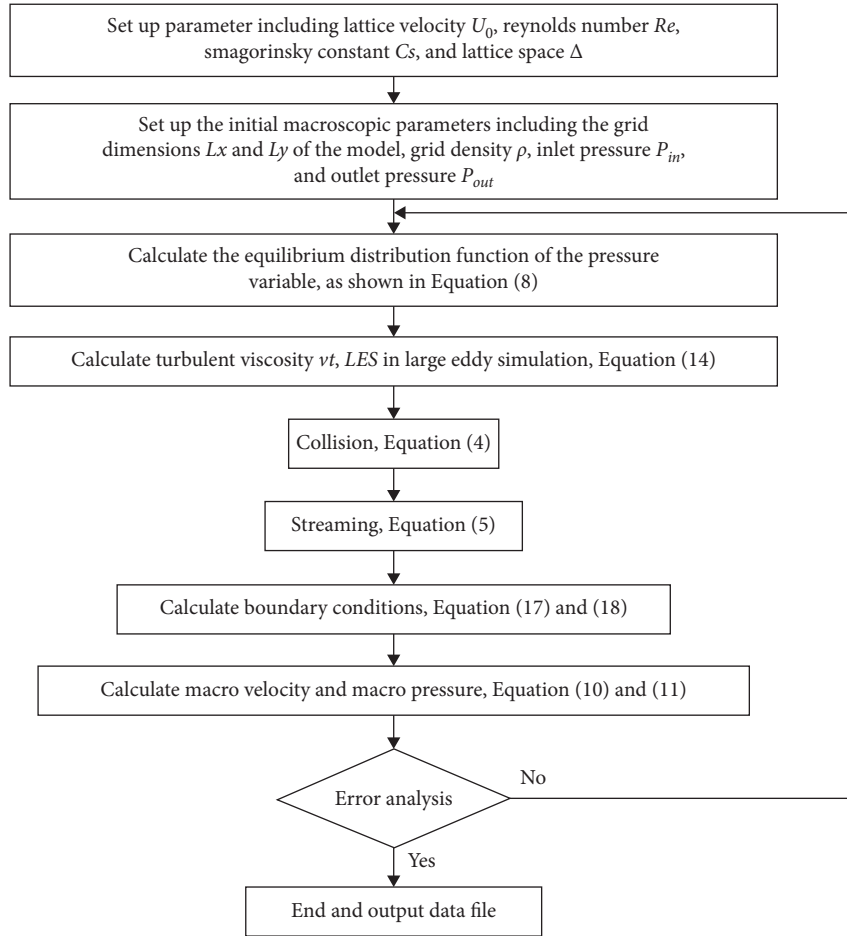
FIGURE 3: LBM Program block diagram.
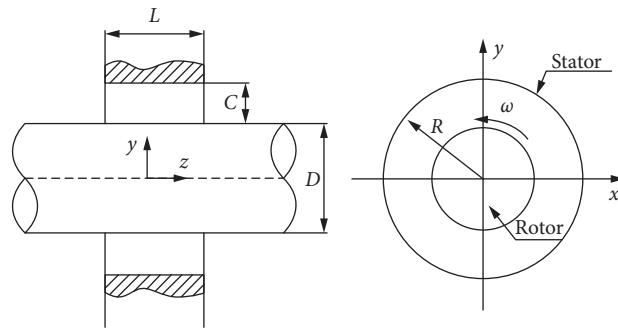


FIGURE 4: Basic geometry of liquid annular seal.

TABLE 1: Geometric parameters of three model seals.

| Model | 1 | 2 | 3 |
|---|---|---|---|
| Reference | Lindsey and Childs [31] | Darden et al. [32] | Marquette et al. [33] |
| Seal clearance $C$ (mm) | 0.076 | 0.53 | 0.11 |
| Seal length $L$ (mm) | 13.13 | 45.7 | 34.93 |
| Seal diameter $D$ (mm) | 76.2 | 91.4 | 76.29 |
| Open area $S$ (mm$^2$) | 18.2 | 152.99 | 26.39 |

TABLE 2: Operating conditions of the model seals.

| Model | 1 | | |
|---|---|---|---|
| Pressure difference (MPa) | 1.38 | 2.41 | 3.45 |
| Inlet velocity (m/s) | 50.44 | 69.91 | 82.96 |
| Rotor speed (rpm) | 10200 | 10200 | 10200 |
| Kinematic viscosity (m$^2$/s) | $5.215e-7$ | $5.215e-7$ | $5.215e-7$ |
| Reynolds numbers | 6038 | 9713 | 12182 |
| Model | 2 | | |
| Pressure difference (MPa) | 9.29 | 11.5 | 12.6 |
| Inlet velocity (m/s) | 130.082 | 144.6 | 151.36 |
| Rotor speed (rpm) | 5500 | 15800 | 5950 |
| Kinematic viscosity (m$^2$/s) | $1.0048e-6$ | $1.0048e-6$ | $1.0048e-6$ |
| Reynolds numbers | 69013 | 76270 | 79835 |
| Model | 3 | | |
| Pressure difference (MPa) | 4.14 | 5.52 | 6.89 |
| Inlet velocity (m/s) | 87.37 | 100.881 | 112.7 |
| Rotor speed (rpm) | 10200 | 10200 | 10200 |
| Kinematic viscosity (m$^2$/s) | $5.215e-7$ | $5.215e-7$ | $5.215e-7$ |
| Reynolds numbers | 18426 | 21277 | 23771 |

transformation equation of lattice pressure $P$ and reference pressure $P_r$ is shown as follows.

In equation (22), $P_c$ is the stagnation point pressure in the lattice unit, and it must take the same value for the stimulating of same model seal. The value of $P_c$ generally takes less than 1 but more than 0.09 for accelerating convergence.

Moreover, as the lattice Reynolds number $Re_{\text{lattice}}$ shown in equation (14), it is equal to the macroscopic Reynolds number $Re$, and it is possible to choose proper values for $U_{\text{lattice}}$ and $\nu_0$ under the condition that $Re_{\text{lattice}}$ equals to $Re$ [35]. Recently, $\nu_0$ remains consistent in different stimulation cases for the same model. Therefore, the value of $\nu_0$ in this work remains the same for the same model seal when stimulations for different operation conditions are conducted. The simulation parameters of the model seals are listed in Table 3.

A grid independence study for each of the three models using seven different sizes of lattices has been carried out, as shown in Figure 5. The simulation time and convergence accuracy are taken into account, the lattice number of Childs' model is chosen as 470,444, Darden's model is chosen as 432,460, and Marquette's model is chosen as 271,846. Leakage error $\varepsilon$ shown in Figure 5 is calculated based on equation (23), where $Q_n$ is the numerical result and $Q_e$ is the experimental result:

$$\varepsilon = \frac{|Q_n - Q_e|}{Q_e} \times 100\%. \tag{23}$$

*3.2. Parameters of FVM.* The calculation results based on FVM which is realized by FLUENT software are compared with the results based on the proposed method in this study. Transient 2D model, 2D coupled solver, and implicit difference scheme are applied. The LES Smagorinsky model is introduced to describe the fluid stress term in the control equations and is discretized with the first-order upwind

style. The convergence condition is that the residuals of all the equations are less than $1 \times 10^{-5}$.

*3.3. Parameters of Empirical Formulas.* As the empirical formulas shown in equation (24) are the most commonly used method for calculating the leakage flow rates of the seals in engineering, in this work, the theoretical results of empirical formulas also act as an important part of the comparisons. In the empirical formulas, $C$ is the seal clearance, $\mu$ is the flow coefficient, $L$ is the seal length, $S$ is the open area of seal clearance, and $Q$ is the leakage of seal. As shown in the above equations, $\mu$ is related to the input rounded coefficient, and the friction coefficient number is determined by the Reynolds number and the surface roughness. The coefficient $\lambda$ generally takes the value between 0.04 and 0.06, and the coefficient $\eta$ takes the value between 0.5 and 0.9.

$$\begin{cases} S = 2\pi RC, \\[2ex] \mu = \dfrac{1}{\sqrt{1 + 0.5\eta + (\lambda L/2C)}}, \\[2ex] Q = \mu S \sqrt{2g(P_{\text{in}} - P_{\text{out}})}. \end{cases} \tag{24}$$

# 4. Results and Discussion

The comparisons of predicted leakage flow rates of three different liquid annular seals under different operating conditions based on LBM, FVM results, empirical formulas, and experiences are conducted and discussed in this section.

*4.1. Results of Model 1.* As shown in Table 4, the simulation results of Model 1 based on LBM, FVM, and empirical formulas are compared with the experimental results conducted by Childs [28]. Since the clearance of the annular seal is small, enlarged velocity contour diagrams at the seal exit

TABLE 3: LBM-LES simulation parameters of the model seals.

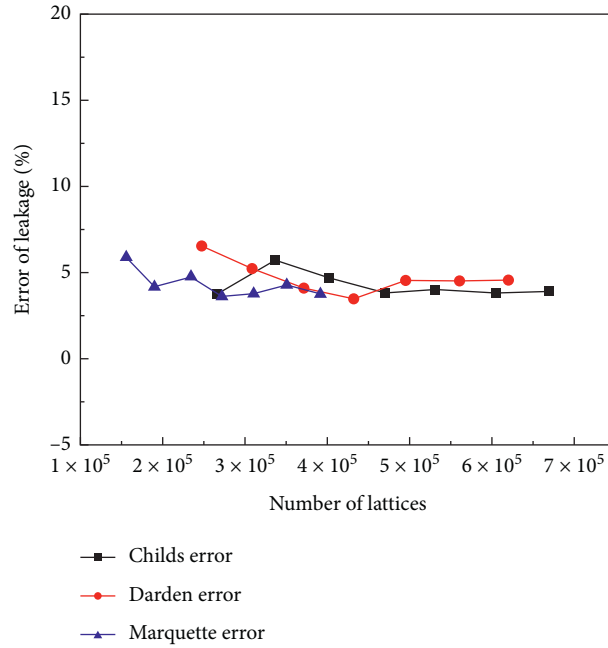| Model | 1 | 2 | 3 |
|---|---|---|---|
| Number of grids in radial direction | 52 | 70 | 29 |
| Number of grids in axial direction | 9047 | 6178 | 9374 |
| Length to height ratio | 172 | 86 | 318 |
| $P_c$ | 0.6 | 0.7 | 0.4 |
| $U_{\text{lattice}}$ | 0.00869, 0.0125, 0.0157 | 0.065, 0.0722, 0.0756 | 0.042, 0.0485, 0.0542 |
| $v_0$ | $6.639e-5$ | $6.639e-5$ | $6.639e-5$ |



FIGURE 5: Grid sensitivity.

TABLE 4: Childs leakage annular seals at different simulate methods.

| Operating conditions | Pressure difference (MPa) | 1.38 | 2.41 | 3.45 |
|---|---|---|---|---|
| Leakage flow rates of LBM (L/s) | | 0.51 | 0.706 | 0.883 |
| Leakage flow rates of FVM (L/s) | | 0.492 | 0.694 | 0.857 |
| Leakage flow rates of empirical formulas (L/s) | | 0.468 | 0.619 | 0.741 |
| Leakage flow rates of test results (L/s) | | 0.492 | 0.7 | 0.864 |
| Leakage flow error of LBM (%) | | 0.362 | 0.799 | 2.16 |

based on LBM under different operating conditions are shown in Figure 6. From Figure 6, it can be found that the fluid velocity increases as the pressure difference increases. In the seal clearance, the fastest fluid velocity is at the center of the clearance. The comparisons show that the empirical formulas are the most time efficient method but with the lowest prediction accuracy of leakage flow rates. The maximum error of the empirical formulas is nearly 15%. LBM and FVM have a good accuracy with a maximum error of less than 3.86% and 6.42%, respectively. For this model, the accuracy of LBM is higher than that of FVM. In contrast with the complex modeling and meshing process of FVM, for different model seals using LBM, only a few initial parameters such as geometric parameters, inlet velocity, and pressure difference need to be changed, which has made LBM more time efficient and more suitable for engineering application.

4.2. Results of Model 2. Experimental results are conducted by Darden et al [32], and the calculation results which are calculated by the three methods for leakage flow rates of Model 2 are shown in Figure 7 and Table 5. It is observed that the leakage rates based on empirical formulas were under-predicted with an error of more than 10% compared to the experimental results. The prediction error of the leakage rate based on FVM is 2.85% under the pressure difference of 9.29 MPa but with error of more than 5% under the other two operating conditions. Among the three methods, LBM has obvious advantages in leakage prediction accuracy, especially under high pressure differences. The prediction error of LBM-LES decreases from 3.48% to 2.32% as the pressure difference increases, while the error of FVM shows an opposite variation.
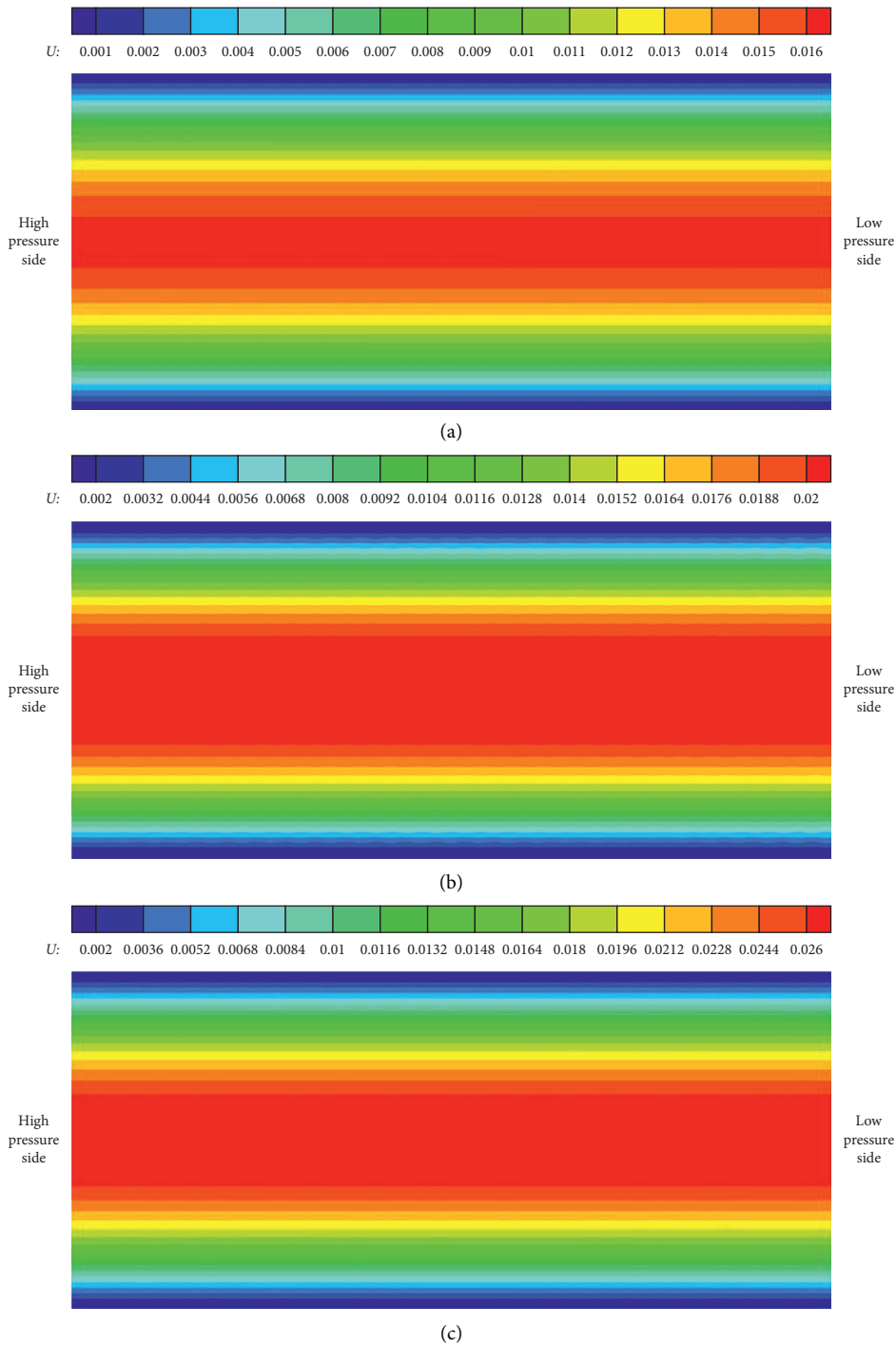
(a)



(b)



(c)

FIGURE 6: Different pressure difference velocity contour using LBM of Model 1. Velocity contour under (a) 1.38 MPa, (b) 2.41 MPa, and (c) 3.45 MPa using LBM.

*4.3. Results of Model 3.* Experimental results are conducted by Marquette et al [33], and the calculation results based on three methods for predicting leakage flow rates of Model 3 are shown in Figure 8 and Table 6. It is observed that the calculation errors of the empirical formula are all around 8%. Calculation errors of FVM decrease with the increasing pressure differences. The maximum error is 12.48%, and the minimum error is 2.55%. By contrast, prediction results based on LBM show good agreement with the experimental results. All of the results have a margin of error of less than 4%. Even more, the prediction error is less than 2% under the pressure difference of 5.52 MPa and 6.89 MPa.
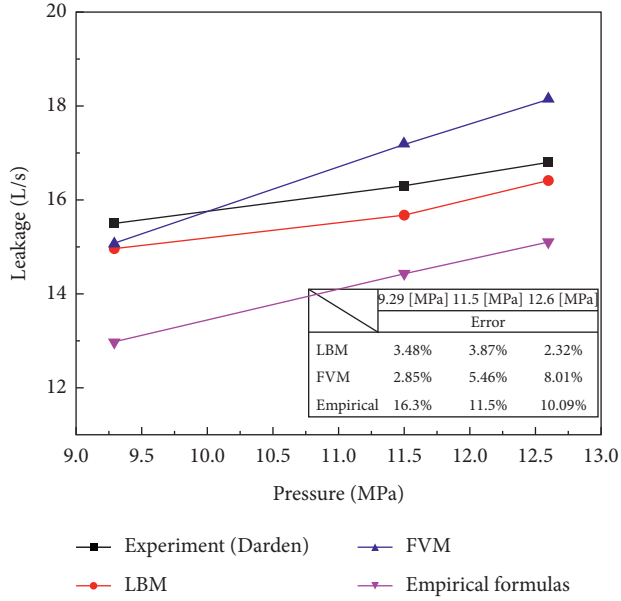
FIGURE 7: Comparisons of leakage flow rates of Model 2 with different methods.

TABLE 5: Darden leakage annular seals at different simulate methods.

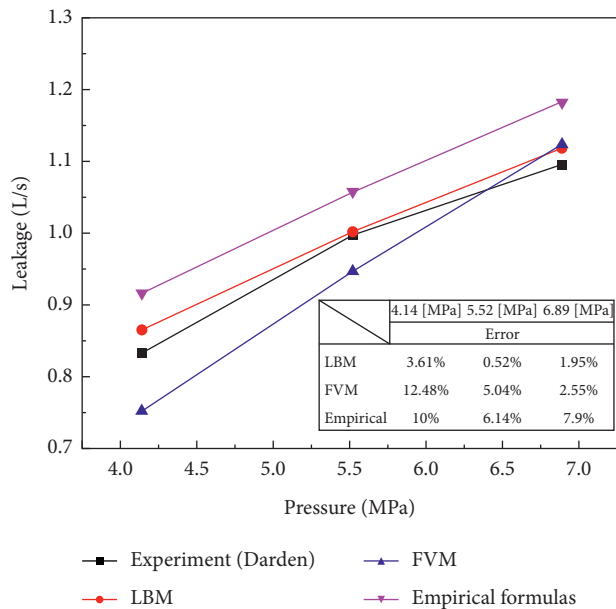| Operating conditions | Pressure difference (MPa) | 9.29 | 11.5 | 12.6 |
|---|---|---|---|---|
| Leakage flow rates of LBM (L/s) | | 14.96 | 15.67 | 16.41 |
| Leakage flow rates of FVM (L/s) | | 15.06 | 17.19 | 18.15 |
| Leakage flow rates of empirical formulas (L/s) | | 12.97 | 14.43 | 15.11 |
| Leakage flow rates of test results (L/s) | | 15.5 | 16.3 | 16.8 |
| Leakage flow error of LBM (%) | | 3.48 | 3.87 | 2.32 |
| Leakage flow error of FVM (%) | | 2.85 | 5.46 | 8.01 |
| Leakage flow error of empirical (%) | | 16.3 | 11.5 | 10.09 |



FIGURE 8: Comparisons of leakage flow rates of Model 3 with different methods.

TABLE 6: Marquette leakage annular seals at different simulate methods.

| Operating conditions | Pressure difference (MPa) | 4.14 | 5.52 | 6.89 |
|---|---|---|---|---|
| Leakage flow rates of LBM (L/s) | | 0.87 | 1.002 | 1.12 |
| Leakage flow rates of FVM (L/s) | | 0.75 | 0.95 | 1.124 |
| Leakage flow rates of empirical formulas (L/s) | | 0.92 | 1.06 | 1.18 |
| Leakage flow rates of test results (L/s) | | 0.83 | 1.00 | 1.09 |
| Leakage flow error of LBM (%) | | 3.61 | 0.52 | 1.95 |
| Leakage flow error of FVM (%) | | 12.48 | 5.04 | 2.55 |
| Leakage flow error of empirical (%) | | 10 | 6.14 | 7.9 |

## 5. Conclusions

In this paper, a 2D LBM calculating model which consists of 2D LES turbulence model, D2G9 velocity model, and nonequilibrium extrapolation scheme is established for predicting of leakage flow rates and static characteristics of liquid annular seals. The leakage rates of three different plain annular seals under three different operating conditions are calculated, and the results of them are compared with the experimental results to prove the validity and accuracy of the proposed model. Comparisons show that all of the prediction errors of the 2D LBM calculating model are less than 5%, some of them even less than 2%, which indicates that the calculating model satisfies the requirements of engineering application better compared with the other commonly used methods. The accuracy of the calculating model for predicting the leakage flow rates of seals is mainly related to the clearance and pressure differences of the model seals. The accuracy decreases with the increasing clearance of the model seals which increases with the increase in pressure difference.

The transformation equation of reference pressure $Pr$ is developed based on the Bernoulli equation for incompressible fluids within annular seals. Reference velocity, reference density, and stagnation point pressure $Pc$ in lattice unit are introduced in this transformation equation, and the optimal value range of $Pc$ for leakage rates predictions of annular seals is proposed.

## Nomenclature

| | |
|---|---|
| $c_s'$: | Physical velocity of sound |
| $\rho'$: | Physical density |
| $H'$: | Physical length |
| $P'$: | Physical pressure |
| $u$: | Physical velocity |
| $C$: | Clearance of seals |
| $L$: | Length of seals |
| $e$: | Eccentricity of the rotor |
| $D$: | Diameter of seals |
| $P_{in}$: | Supply pressure of seal |
| $P_{out}$: | Exit pressure of seal |
| $\Omega$: | Rotor whirl velocity |
| $\omega$: | Rotor angular velocity |
| $\nu_0$: | Lattice kinematic viscosity |

$\nu_{t,\text{LES}}$: Eddy viscosity
$\tau$:       Relaxation time
$M$:      Collision operator
$\gamma$:      Collision frequency
$c_s$:      Lattice velocity of sound
$c$:       Lattice velocity
$\rho$:       Lattice density
$P$:       Lattice pressure
$H$:      Lattice length
$u_r$:      Reference velocity
$\rho_r$:      Reference density
$H_r$:      Reference length
$P_c$:      Stagnation point pressure
$P_r$:      Reference pressure
$Q$:       Quantity of flow
$Qn$:     Numerical result of leakage
$Qe$:     Experimental result of leakage
$\mu$:       Flow coefficient
$\eta$:       Rounded coefficient
$\lambda$:       Friction coefficient number.

## Data Availability

The numerical and experimental data used to support the findings of this study are included within the article.

## Conflicts of Interest

The authors declare that they have no conflicts of interest.

## Acknowledgments

## References

[1]  B. R. Kucinschi and A. A. Afjeh, "A lattice Boltzmann approach to fluid film lubrication," *Journal of Tribology*, vol. 132, no. 2, pp. 0217051–0217057, 2010.

[2]  H. M. Kim, D. Kim, W. T. Kim, P. S. Chung, and M. S. Jhon, "Langmuir slip model for air bearing simulation using the lattice Boltzmann method," *IEEE Transactions on Magnetics*, vol. 43, no. 6, pp. 2244–2246, 2007.

[3]  A. J. Ramirez, A. M. Guzman, and R. A. Escobar, "Flow dynamics characteristics in micro and nano length scales devices with the lattice Boltzmann method: the air bearing problem," *ASME International Mechanical Engineering Congress and Exposition*, vol. 13, no. 1, pp. 611–620, 2008.

[4]  A. Posa and A. Lippolis, "A LES investigation of off-design performance of a centrifugal pump with variable-geometry diffuser," *International Journal of Heat and Fluid Flow*, vol. 70, pp. 299–314, 2018.

[5]  X. Li, P. Gao, Z. Zhu, and Y. Li, "Effect of the blade loading distribution on hydrodynamic performance of a centrifugal pump with cylindrical blades," *Journal of Mechanical Science and Technology*, vol. 32, no. 3, pp. 1161–1170, 2018.

[6]  Q. Si, P. Dupont, A.-C. Bayeul-Lainé, A. Dazin, O. Roussette, and G. Bois, "Static pressure recovery analysis in the vane island diffuser of a centrifugal pump," *Journal of Mechanical Science and Technology*, vol. 30, no. 2, pp. 549–556, 2016.

[7]  L. S. Andres, T. C. Wu, H. Maeda et al., "A computational fluid dynamics modified bulk flow analysis for circumferentially shallow grooved liquid seals," *Journal of Engineering for Gas Turbines and Power: Transactions of the ASME*, vol. 140, no. 1, 2018.

[8]  E. Saber and K. M. Abdou, "Effect of lateral misalignment on performance of a stationary and rotating labyrinth seals," *Alexandria Engineering Journal*, vol. 58, no. 1, pp. 27–38, 2019.

[9]  E. Saber, K. M. Abdou, and R. Afify, "Effect of shaft eccentricity on dynamic characteristics for different geometries of stationary labyrinth seals," *Alexandria Engineering Journal*, vol. 59, no. 1, pp. 61–75, 2020.

[10] K. Nagai, S. Kaneko, H. Taura et al., "Numerical and experimental analyses of static characteristics for liquid annular seals with helical grooves in seal stator," *Journal of Tribology*, vol. 140, no. 3, 2018.

[11] H. Yu and S. S. Girimaji, "Near-field turbulent simulations of rectangular jets using lattice Boltzmann method," *Physics of Fluids*, vol. 17, no. 12, pp. 125106–125117, 2005.

[12] S. Succi, G. Amati, and R. Benzi, "Challenges in lattice Boltzmann computing," *Journal of Statistical Physics*, vol. 81, no. 1-2, pp. 5–16, 1995.

[13] C. M. Teixeira, "Incorporating turbulence models into the Lattice-Boltzmann method," *International Journal of Modern Physics C*, vol. 9, no. 8, pp. 1159–1175, 1998.

[14] S. Hou, J. Sterling, S. Chen et al., "A Lattice Boltzmann subgrid model for high Reynolds number flows," *Fields Institute Communications*, vol. 6, pp. 151–166, 1996.

[15] S. L. Hu, *Numerical Research on Aerodynamic Control Measures of the Long-Span Bridge*, Central South University, Nanjing, China, 2010.

[16] K. N. Premnath, M. J. Pattison, and S. Banerjee, "An investigation of the lattice Boltzmann method for large eddy simulation of complex turbulent separated flow," *Journal of Fluids Engineering*, vol. 135, no. 5, pp. 051401 1–051401 12, 2013.

[17] A. Schneider, D. Conrad, and M. Boehle, "Lattice boltzmann simulation of the flow field in pump intakes: a new approach," *ASME 2013 Fluids Engineering Division Summer Meeting*, pp. 49–61, Incline Village, Reno, NV, USA, 2013.

[18] S.-C. Chang, Y.-T. Yang, C. o.-K. Chen, and W.-L. Chen, "Application of the lattice Boltzmann method combined with large-eddy simulations to turbulent convective heat transfer," *International Journal of Heat and Mass Transfer*, vol. 66, no. 6, pp. 338–348, 2013.

[19] D. Hamane, O. Guerri, and S. Larbi, "Investigation of flow around a circular cylinder in laminar and turbulent flow using the lattice Boltzmann method," *Proceedings of the International Conference on Numerical Analysis and Applied Mathematics*, vol. 1648, pp. 513–520, 2015.

[20] A. G. Eitel, M. Meinke, and W. Schroeder, "A lattice Boltzmann method with hierarchically refined meshes," *Computers & Fluids*, vol. 75, no. 6, pp. 127–139, 2013.

[21] N. Nadim, T. T. Chandratilleke, and M. J. N. Krause, "LBM-LES modelling of low reynolds number turbulent flow over NACA0012 aerofoil," in *Proceedings of the 3rd Symposium On Fluid-Structure-Sound Interactions And Control*, pp. 205–210, Perth, Australia, January 2016.

[22] Z. L. Guo and C. G. Zheng, *Theory and Applications of Lattice Boltzmann Method*, Wiley, Beijing, China, 2009.

[23] A. D. WolfGladrow, *Lattice Gas Cellular Automata and Lattice Boltzmann Models*, Springer, Berlin, Germany, 2000.

[24] T. Kataoka and M. Tsutahara, "Lattice Boltzmann model for the compressible Navier-Stokes equations with flexible specific-heat ratio," *Physical Review E*, vol. 69, no. 3, 2004.

[25] L. M. Yang, C. Shu, and J. Wu, "A moment conservation-based non-free parameter compressible lattice Boltzmann model and its application for flux evaluation at cell interface," *Computers & Fluids*, vol. 79, pp. 190–199, 2013.

[26] L. M. Yang, C. Shu, and J. Wu, "Extension of lattice Boltzmann flux solver for simulation of 3D viscous compressible flows," *Computers & Mathematics with Applications*, vol. 71, no. 10, pp. 2069–2081, 2016.

[27] Y. H. Qian, D. D'Humières, and P. Lallemand, "Lattice BGK models for Navier-Stokes equation," *Europhysics Letters (EPL)*, vol. 17, no. 6, pp. 479–484, 1992.

[28] Z. Guo, B. Shi, and N. Wang, "Lattice BGK model for incompressible Navier-Stokes equation," *Journal of Computational Physics*, vol. 165, no. 1, pp. 288–306, 2000.

[29] S. Chapman, T. G. Cowling, and D. Park, *The Mathematical Theory of Non-uniform Gases*, Cambridge University Press, Cambridge, UK, 3rd edition, 1970.

[30] Z. L. Guo and B. C. Shi, "Non-equilibrium extrapolation method for velocity and pressure boundary conditions in the lattice Boltzmann method," *Chinese Physics B: English*, vol. 11, no. 4, pp. 366–374, 2002.

[31] W. T. Lindsey and D. W. Childs, "The effects of converging and diverging axial taper on the rotordynamic coefficients of liquid annular pressure seals: theory versus Experiment," *Journal of Vibration and Acoustics*, vol. 122, no. 2, pp. 126–131, 2000.

[32] J. M. Darden, E. M. Earhart, and G. T. Flowers, "Comparison of the dynamic characteristics of smooth annular seals and damping seals," *Journal of Engineering for Gas Turbines and Power*, vol. 123, no. 4, pp. 857–863, 1999.

[33] O. R. Marquette, D. W. Childs, and L. San Andres, "Eccentricity effects on the rotordynamic coefficients of plain annular seals: theory versus experiment," *Journal of Tribology*, vol. 119, no. 3, pp. 443–447, 1997.

[34] Y. L. He, *Lattice Boltzmann Method, Theory and Applications*, Science Press, Beijing, China, 2009.

[35] A. A. Mohamad, *Lattice Boltzmann Method*, Springer, Berlin, Germany, 2011.